Chemical Science

ROYAL SOCIETY OF CHEMISTRY

EDGE ARTICLE

View Article Online
View Journal | View Issue

Cite this: *Chem. Sci.*, 2023, **14**, 8288

All publication charges for this article have been paid for by the Royal Society of Chemistry

Fragment expansion with NUDELs – poised DNA-encoded libraries†

Catherine L. A. Salvini,[a] Benoit Darlot,[bc] Jack Davison,[a] Mathew P. Martin,[d] Susan J. Tudhope,[d] Shannon Turberville,[d] Akane Kawamura,[bc] Martin E. M. Noble,[d] Stephen R. Wedge,[d] James J. Crawford [e] and Michael J. Waring *[a]

Optimisation of the affinity of lead compounds is a critical challenge in the identification of drug candidates and chemical probes and is a process that takes many years. Fragment-based drug discovery has become established as one of the methods of choice for drug discovery starting with small, low affinity compounds. Due to their low affinity, the evolution of fragments to desirable levels of affinity is often a key challenge. The accepted best method for increasing the potency of fragments is by iterative fragment growing, which can be very time consuming and complex. Here, we introduce a paradigm for fragment hit optimisation using poised DNA-encoded chemical libraries (DELs). The synthesis of a poised DEL, a partially constructed library that retains a reactive handle, allows the coupling of any active fragment for a specific target protein, allowing rapid discovery of potent ligands. This is illustrated for bromodomain-containing protein 4 (BRD4), in which a weakly binding fragment was coupled to a 42-member poised DEL *via* Suzuki–Miyaura cross coupling resulting in the identification of an inhibitor with 51 nM affinity in a single step, representing an increase in potency of several orders of magnitude from an original fragment. The potency of the compound was shown to arise from the synergistic combination of substructures, which would have been very difficult to discover by any other method and was rationalised by X-ray crystallography. The compound showed attractive lead-like properties suitable for further optimisation and demonstrated BRD4-dependent cellular pharmacology. This work demonstrates the power of poised DELs to rapidly optimise fragments, representing an attractive generic approach to drug discovery.

Received 3rd March 2023
Accepted 11th July 2023

DOI: 10.1039/d3sc01171b

rsc.li/chemical-science

Introduction

Fragment-based lead generation[1–3] and DNA-encoded library screening[4–6] are two important technologies for identifying ligands for protein targets in chemical biology and medicinal chemistry. The primary rationale for fragment-based approaches is that by screening small (typically <350 Da) compounds, a much greater range of chemical structures can be represented with fewer compounds, making screening more efficient and increasing the chances of finding hits.[7,8] Because these hits are small, they typically bind with low affinity often in the millimolar range, necessitating sensitive biophysical techniques (NMR, SPR, X-ray crystallography) to detect their binding. It can take considerable time and effort to develop them into compounds that have high enough affinity to achieve activity in biochemical assays and to carry out target validation studies, which are critical steps in the development of chemical probes and therapeutics.

In contrast, DNA-encoded libraries (DELs) consist of collections of compounds covalently linked to unique DNA-oligonucleotides that encode their chemical structure. Through combinatorial synthesis, DELs allow the screening of vast numbers (often billions) of pooled compounds.[9] They can be screened very efficiently by affinity selection, subsequent PCR amplification of the bound species and DNA sequencing.[5] Synthesis of the molecules identified in the selection without the DNA-tags is then carried out to confirm the hits using traditional assays. Despite the ability to screen such large numbers of compounds, it is still not feasible to significantly cover chemical diversity at the higher molecular weight ranges that are typical of DELs. While the exact size of this chemical space is difficult to estimate, it is believed to be extremely vast,

[a]*Cancer Research Horizons Therapeutic Innovation Newcastle Drug Discovery Group, Chemistry, School of Natural and Environmental Sciences, Newcastle University, Bedson Building, NE1 7RU, UK. E-mail: mike.waring@ncl.ac.uk*

[b]*Chemistry, School of Natural and Environmental Sciences, Newcastle University, Bedson Building, NE1 7RU, UK*

[c]*Department of Chemistry, University of Oxford, 12 Mansfield Road, Oxford OX1 3TA, UK*

[d]*Cancer Research Horizons Therapeutic Innovation Newcastle Drug Discovery Group, Translational and Clinical Research Institute, Newcastle University, Paul O'Gorman Building, NE2 4HH, UK*

[e]*Genentech Inc., 1 DNA Way, South San Francisco, California, 94080, USA*

† Electronic supplementary information (ESI) available: Detailed experimental procedures for synthesis and selection of the libraries and off-DNA synthesis, protein production SPR testing, crystallography and cellular pharmacology. See DOI: https://doi.org/10.1039/d3sc01171b

with estimates ranging from 10^{60} to 10^{200}.[10,11] Such libraries should still be focused on biologically relevant chemical space, *i.e.* consisting mainly of compounds with lead-like physicochemical properties and free of undesirable functionality. This places significant constraints on library design. In addition, subsequent optimisation of hits from DEL screens often requires significant reengineering of their chemical structures, which again can be inefficient and time consuming.

We proposed that it would be possible to significantly accelerate the process of optimising fragment hits for any given protein by preparing a poised DNA-encoded library in which every member contained a functional handle that allowed the attachment of an active fragment (Fig. 1a). Such a poised library would then be available to couple with active fragments for any selected target in a single step. A subsequent fragment screen would generate fragment hits specific for a chosen target (Fig. 1b). A selected fragment hit derivatised with a complementary reactive group would then be coupled to the poised library, producing a DEL that was focused on the chosen target (Fig. 1c). By employing two synthesis cycles in the poised library synthesis, this would maintain the optimal profile of lead-likeness, library fidelity, synthesis yields and chemical diversity in the final libraries once the active fragment is coupled, as well as maintaining the required signal-to-noise ratios in the selections.[12,13]

The focused DEL would be screened by affinity selection to identify higher affinity, elaborated ligands (Fig. 1d). This would enable the rapid expansion of fragment hits to compounds with potentially much increased affinity in a single operation without the need for the stepwise fragment growing process, currently the most commonly adopted approach to FBLG.[14] Alternatively, this concept could be viewed as a flexible means of focusing a DEL on chemical space that was directly relevant to a selected protein target. These poised libraries we term "NUDELs" because of their origin at Newcastle University.

The ESAC approach[15–17] facilitates the discovery of hits for proximal binding pockets on a protein. Similar approaches have been applied to the discovery of ligands with applications in selective delivery of therapeutic radionuclides.[18] Generated hits have then been connected by flexible linker to give probe-like compounds, to our knowledge this has yet to be used to yield drug-like molecules. The NUDEL methodology by contrast provides direct covalent connection between the hit fragment and expansion library, resulting directly in lead-like compounds, without the need for further iterative optimisation.

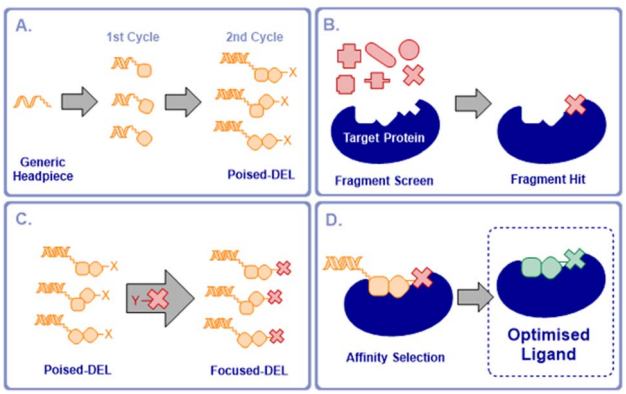

Fig. 1 Concept of a poised DEL for fragment elaboration. (a) Synthesis of a 2-cycle poised DEL with a reactive group X; (b) fragment screen to identify active fragments; (c) coupling of the poised DEL to a selective fragment derivatised with complementary reactive group Y to produce a focused DEL; (d) affinity selection of focused DEL to select optimised ligands.

Results and discussion

Synthesis of the poised DNA-encoded library

The first NUDEL was designed based on two sequential amide couplings involving coupling of a set of Fmoc-protected amino acids to an amino-derivatised DNA-head piece in cycle 1, followed by Fmoc-deprotection and second amide coupling with a set of aryl halide-containing acids. Libraries of this design could then incorporate any active fragment for which a derivative was available with a functional group that allowed coupling with the halide. Commonly used reactions of this type, such as Suzuki–Miyaura[19,20] and Buchwald–Hartwig[21] reactions, have been recently shown to work efficiently on DNA-tagged substrates.

The library components were selected based on diversity of shape and chemical functionality such that the resulting test compounds would represent diverse lead-like structures (Fig. 2a). Seven Fmoc amino acids, consisting of canonical amino acids alanine, valine and phenylalanine, pyrrolidine-3 carboxylic acid and aniline derivatives 3- and 4-aminobenzoic acid and (4-methylamino)benzoic acid, were selected for cycle 1. Six aryl halide-containing acids: 3- and 4-iodobenzoic acid, (4-iodophenyl)acetic acid 5-iodonicotinic acid, 2-(6-bromopyridin-3-yl)acetic acid and 2-(4-bromo-1*H*-pyrazol-1-yl)acetic acid, were selected for cycle 2. Thus, the final library would contain a variety of hydrogen bond donor, acceptor, aromatic and lipophilic functionality, which make up the majority of pharmacophoric interactions, with differing overall shapes that present different relative orientations of the components. Incorporation of additional hydrogen bond donors was avoided in the building block variation due to their necessary presence in the amide linkages used in the assembly of the library.

Through the DEL methodology, large numbers of compounds become synthetically achievable in parallel. However, one of the major disadvantages of working with DNA-conjugated compounds is that the removal of side products is difficult. Underpinning the fidelity of the library is the requirement that reactions used in its synthesis proceed in high conversion to the intended product. This ensures that the compound structure associated with each label is correct, as side products or incomplete reactions give rise to multiple products attached to the same sequence. To ensure the NUDEL was of high fidelity, examples of amide coupling conditions for compounds **1a–c** with headpiece **6** were optimised to the highest conversions, before further expanding for the selected library building blocks. Though this proposed library may be small when compared to DELs in the published literature, it contains numbers of analogues that are comparable to those used in generation of SAR in a fragment growing campaign and

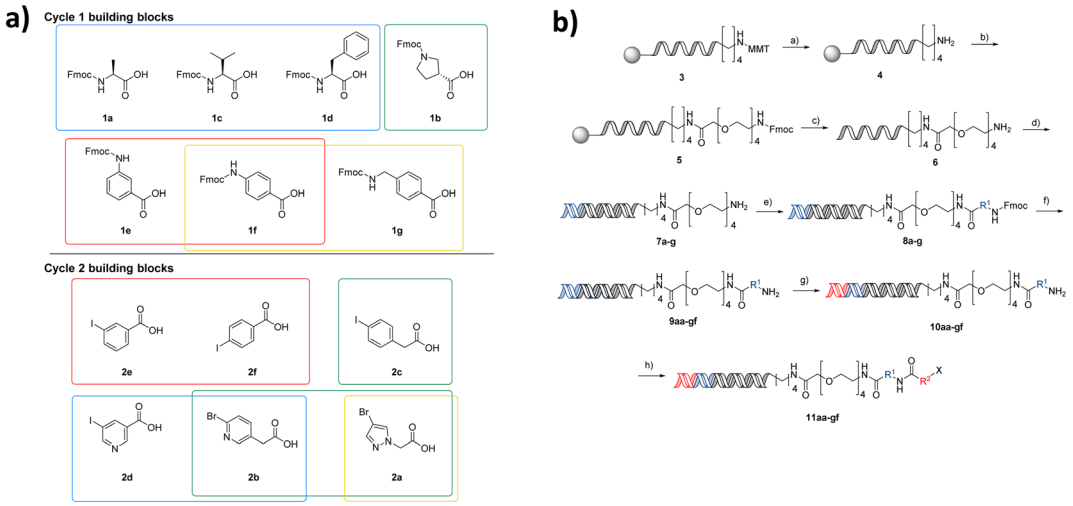

Fig. 2 Poised NUDEL library design and synthesis. (a) Building block selection, cycle 1: blue, canonical amino acids; green, 2° amine; red, aniline derivatives and positional isomers; yellow, increased spacer length; cycle 2: red, positional isomers; green, increased spacer; blue, 6 membered heterocycles; yellow, 5-membered heterocycles; (b) NUDEL synthesis (first letter referring to BB1 a = 1a, second letter referring to BB2 a = 2a *etc.*), reagents and conditions: (a) TCA, DCM; (b) DMF, DIPEA, HATU, Fmoc-PEG acid; (c) $MeNH_2$, NH_3, H_2O; (d) (i) PNK, PNK buffer (ii) ligase, ligase buffer; (e) DMTMM, Fmoc-amino acid borate buffer pH 9.4, H_2O/DMF; (f) 10% piperidine, H_2O; (g) (i) PNK, PNK buffer (ii) ligase, ligase buffer; (h) DMT-MM, aryl-acid, H_2O/DMF.

allows them to be accessed far more rapidly than *via* traditional medicinal chemistry synthesis strategies. Working with a small-scale library afforded the ability to conduct thorough validation experiments for each individual coupling and stage of library construction. The purity and conversion of the library synthesis were prioritised over scale in this first proof of concept, to ensure the fidelity of the library.

After a period of optimisation, the library synthesis protocol involved on-resin monomethoxytrityl deprotection of a hexylamino-tagged DNA adapter sequence, followed by HATU-mediated coupling of a PEG-4-linker bearing an Fmoc protected amine (Fig. 2b). Concomitant Fmoc deprotection and cleavage from the resin was achieved by methylamine treatment. The resulting headpiece was annealed with a complementary DNA strand and the building block 1 codons attached by enzymatic ligation. The Fmoc amino acids in cycle 1 were incorporated by DMTMM coupling in borate buffer, followed by deprotection to yield the 7 intermediate amines. These intermediates were pooled, and the resulting mixture split into 6 wells. Codon 2 ligation was then carried out followed by a second DMTMM-mediated acylation of the cycle 2 halide-containing acids, resulting in a fully encoded library of 42 aryl halides (**11aa–gf**), poised for coupling of active fragments. Although this library is small by DELs standards, synthesis of matrices of compounds in such a manner in a traditional fragment growing campaign would be far more resource intensive. Additionally, working on a small scale initially provided the opportunity to confirm all transformation combinations employed in the NUDEL construction.

Coupling of an active fragment

To demonstrate the use of the NUDEL to generate a focused library for fragment expansion, we selected bromodomain-containing protein 4 (BRD4) as a test case. 3,5-Dimethylisoxazole is a known active fragment binder of BRD4.[22] We proposed that the NUDEL aryl halides could be derivatised by coupling to the corresponding boronic acid of dimethyl isoxazole *via* on-DNA Suzuki–Miyaura cross-coupling,[19,20] thus providing a BRD4 focused library.

To establish the coupling of dimethylisoxazole boronic acid to the library, a potentially challenging coupling due to the presence of the heterocyclic system and sterically hindering bis-*ortho*-methyl substitution, a model DNA substrate containing the adapter sequence, was used as a trial reaction (Fig. 3a). Micellar-mediated Suzuki–Miyaura conditions performed very well with this substrate, furnishing the coupled dimethylisoxazole with 100% conversion, giving confidence that the BRD4 fragment could be coupled efficiently on-DNA. A sample of the NUDEL was subjected to the same coupling conditions resulting in the BRD4 targeted library.

Affinity selection against BRD4

The targeted library was incubated with immobilised BRD4 (first bromodomain, BD1) protein in the presence of DNA-linked version of the established BRD4 ligand JQ1 (ref. 23) as a positive control. After washing to remove non-binders, the protein was denatured, and the sample subjected to 40 cycles of PCR amplification and next generation sequencing (>150 000 reads). The resulting output was analysed to assess the frequency of occurrence of each building block codon and their enrichment relative to the starting library. Remarkably, this highlighted a specific combination of cycle 1 codon (ACTATGGA) with cycle 2 codon (CTTAGAGC), corresponding to alanine and methyl-amidopyrazole respectively, which occurred significantly more times (11-fold) than any other sequence and was comparable to the enrichment of the JQ1 derived control, spiked into the library

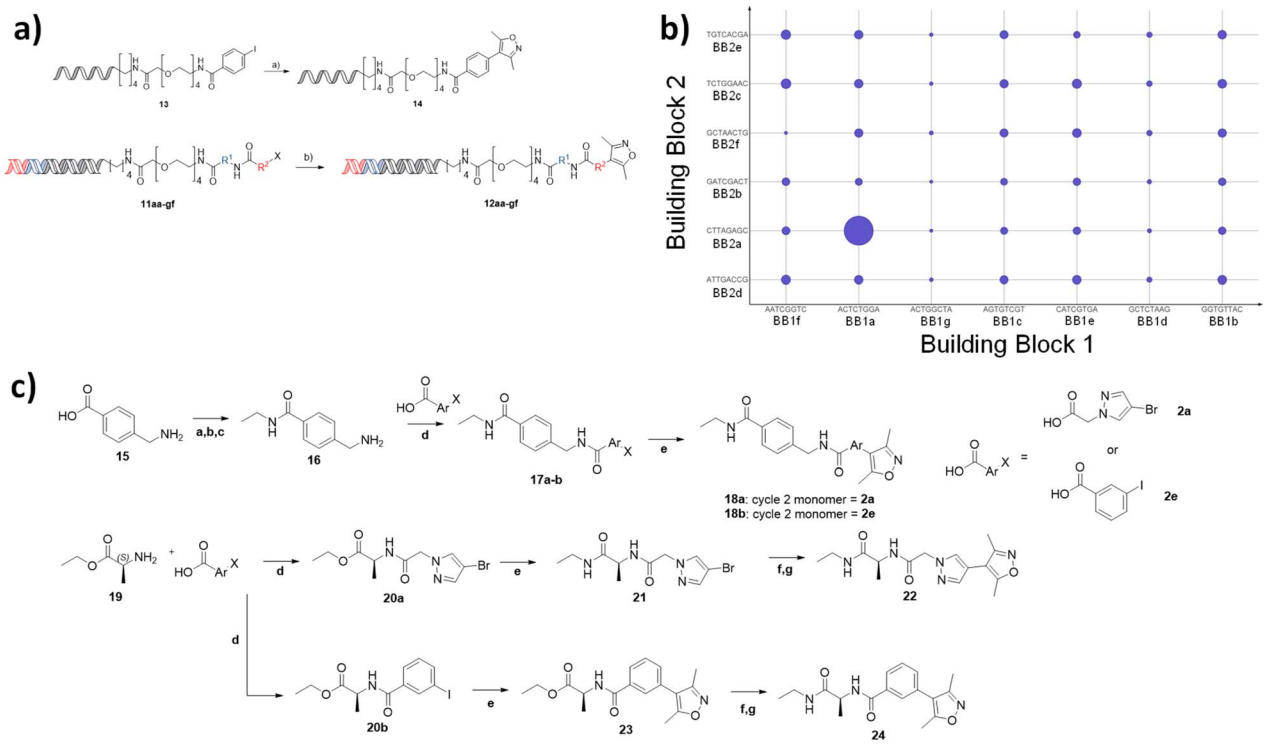

Fig. 3 (a) Coupling of the isoxazole fragment to a model substrate, showing confirmation of Suzuki coupling on DNA, and coupling to the full NUDEL, reagents: (a) Pd(dtbpf)Cl_2, K_3PO_4, H_2O/THF, TPGS-750M 2.5%, 3,5-dimethyl-4-(4,4,5,5-tetramethyl-1,3,2-dioxaborolan-2-yl)isoxazole, (b); (j) Pd(dtbpf)Cl_2, 2% TPGS-750-M, K_3PO_4, H_2O/THF; (b) Selection of targeted library against BRD4 showing enrichment of sequences by size of the points, broken down by building block 1 (*X*-axis) and building block 2 (*Y*-axis) codons; (c) Off-DNA synthesis of 4 compounds. **18a** synthesised from **2a**, **18b** synthesised from **2e**. Reagents: (a) TFAA; (b) $SOCl_2$; (c) NH_2Et in THF 2M; (d) HATU, DIPEA, DCM (e) Pd(dtbpf)Cl_2, Cs_2CO_3, Diox./H_2O 10 : 1, 3,5-dimethyl-4-(4,4,5,5-tetramethyl-1,3,2-dioxaborolan-2-yl)isoxazole; (f) LiOH, THF/H_2O 1 : 1; (g) HATU, DIPEA, DCM, NH_2Et in THF 2 M.

at the concentration of a representative library member (Fig. 3b). Interestingly, neither codon appeared significantly enriched in any other combination. Together, this suggested that compound **22** would be a potent BRD4 ligand and that the combination of **1a** and **2a**, rather than either motif individually, resulted in a synergistic and multiplicative gain in affinity.

Off-DNA hit confirmation

To confirm the synergistic finding, a 'matched square' of compounds consisting of compound **22**, which corresponded to the hit, **24**, which contained **1a** (active cycle 1 monomer) and **2e** (representative non-enriched cycle 2 monomer), **18a** containing **1g** (representative non-enriched cycle 1 monomer) with **2a** (enriched cycle 2 monomer) and finally **18b** (both non-enriched monomers) were selected for off-DNA synthesis and evaluation (Fig. 3c).

Compounds **18a,b** were synthesised from 4-(aminomethyl) benzoic acid **15** by formation of the primary ethyl amide *via* a protection and deprotection of the amine as the trifluoroacetamide. Subsequent amide coupling to the appropriate cycle 2 monomer and incorporation of the dimethyl isoxazole warhead *via* Suzuki cross-coupling resulted in the desired off-DNA compounds **18a,b** (Fig. 3c). **22** and **24** were obtained in a similar manner, first coupling alanine ethyl ester **19**, with either **2a**, **2e**, followed by Suzuki cross coupling to install the isoxazole. Ester hydrolysis and amide coupling gave the final ethyl amide products **22** and **24**.

SAR analysis

The K_d of **18a**, **18b** and **22** and **24** were evaluated *via* SPR analysis for binding to BRD4 BD1. Gratifyingly, hit compound **22**, had a K_d of 51 nM (Fig. 4a). In contrast the affinities of **18a**,**18b** and **24** were 35 μM, 2.5 μM, and 15 μM, respectively, *i.e.* two to three orders of magnitude less potent (Fig. 4b). This result is consistent with the enrichment observed during the selection and provides evidence that the enrichment from the on-DNA selection depends on the affinity of the compounds. It shows that it is the combination of the alanine and the pyrazolylacetamide moieties, rather than either of them in isolation that is responsible for the dramatic gain in affinity. This highlights a distinct advantage of this approach over traditional fragment growing. It would not be possible to identify this unique, synergistic combination of substructures without synthesising every combination, something that is essentially prohibitive for analogues synthesised off-DNA. Moreover, using fragment growing approaches, this combination could not be identified because the pyrazoleacetamide species would not be identified as beneficial when lacking the cycle 2 alanine and so would not have been selected for subsequent elaboration. The use of the NUDEL, which contains every possible combination

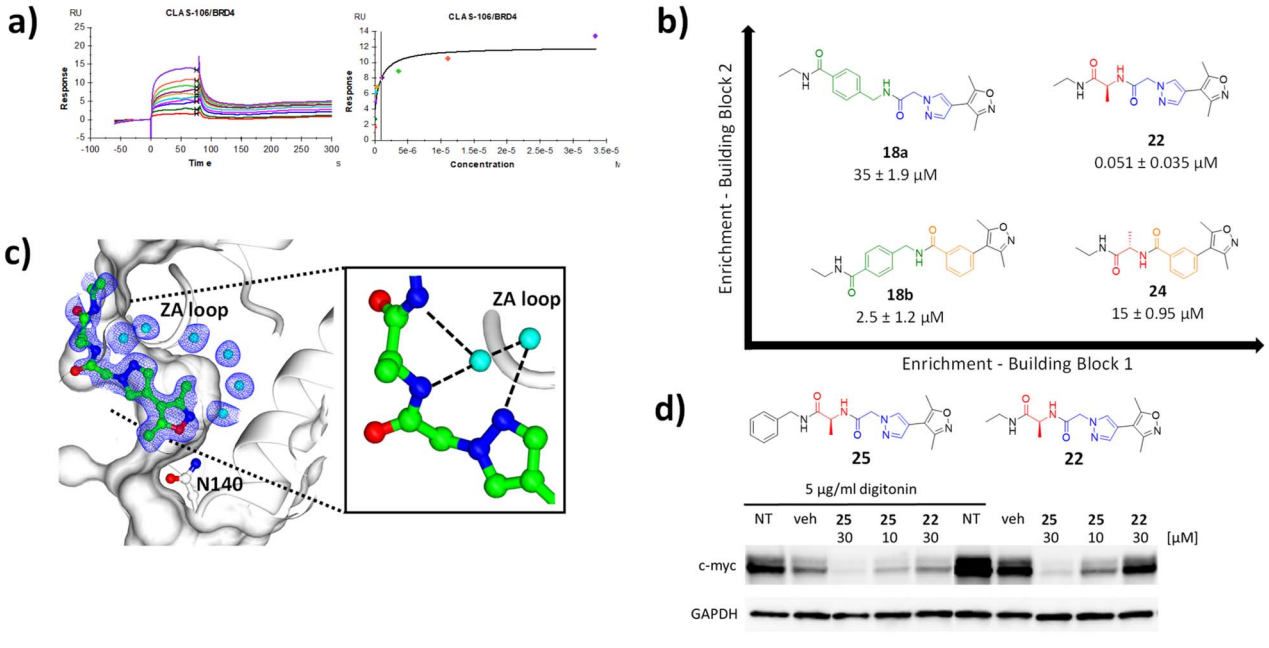

e)

Compound	$LogD_{7.4}$	Solubility	Microsomal Cl_{int} (r/h)	Hepatocyte Cl_{int} (r/h)	MDCK A to B Papp WT / MDR1)
22	0.9	39 μM	<6.1 / <3.9 $mLmin^{-1}kg^{-1}$	11 / 4.1 $mLmin^{-1}kg^{-1}$	3.7 / 1.1 nms^{-1}

Fig. 4 (a) SPR sensograms for **22** against BRD4; (b) matched square of compounds showing increased potency with increased selection enrichment; (c) X-ray crystal structure of **22** bound to BRD4 BD1 (pdb code 8C11); (d) western blot analysis of downregulation of c-Myc in MM.1S cells by compounds **22** and **25** in the presence and absence of digitonin, compared to non-treated (NT) and vehicle (veh) treated cells relative to GAPDH loading control; (e) ADMET profile of **22**.

of the selected substructures, makes the discovery of such synergistic combinations of groups facile.

Characterisation of the binding mode of **22** (CLAS-106) was achieved by solving the crystal structure in complex with BRD4 (Fig. 4c). The crystal structure of the BRD4 complex was determined at 1.8 Å resolution and, as expected, **22** was observed to interact with the KAc recognition site. The oxygen of the isoxazole moiety forms a hydrogen bond with the conserved Asn-140, and a conserved water mediated a hydrogen bond between the nitrogen of the isoxazole and Tyr-97. The pyrazole core is sandwiched between the Pro-82 of the WPF shelf and Leu-92 of the ZA-loop, with a key hydrogen bond formed between a conserved structural water and the main chain of Pro-86 and Gln-85 of the ZA-loop. The extended pyrazole core, a product of cycle 2 synthesis, is further stabilised through additional water mediated hydrogen bonding network involving the main chain of Asp-86. This provides an explanation for the synergistic increase in potency from the combination of the pyrazole and alanine, in that it provides a unique relative orientation of the three critical groups to form complementary hydrogen bonds to the two adjacent structural water molecules.

ADME and cellular pharmacology of 22

To confirm the activity of **22** in a cellular context, human multiple myeloma MM.1S cells were treated with compound. Consistent with the high polarity of the compound, and hence expected low permeability and significant efflux, cells required permeabilisation with digitonin to show activity. In the presence of digitonin, **22** showed downregulation of c-Myc, an established downstream pharmacodynamic marker of BRD4 inhibition[24] at a concentration of 30 μM (Fig. 4d). A more lipophilic, cell permeable analogue **25** (benzyl amide derivative) showed downregulation of c-Myc in a concentration dependent manner in both the presence and absence of digitonin.

The log *D* value for compound **22** was 0.90, thus a lipophilic ligand efficiency of 6.4, which is consistent with a high quality lead compound (Fig. 4e).[25] It had high solubility and low *in vitro* clearance in human and rat microsomes and hepatocytes. As expected, and consistent with the cellular activity, permeability in MDCK cell was low without evidence of MDR1-mediated efflux. Overall, compound **22** is a high-quality technical profile with scope for facile further optimisation.

Methods

Synthesis of the NUDEL

Amide coupling. A solution of DNA HP-1 (1.0 mM) was pipetted into a PCR tube, to which was added pH 9.4 borate buffer (150 mM, 50 μL), amino acid in DMF (150 mM, 12.6 μL), and freshly prepared DMT-MM in water (250 mM, 7.6 μL). Each well was vortexed for 10 seconds and left to shake for 6 hours. A second addition of DMT-MM solution (250 mM, 7.6 μL) was carried out and the mixture allowed to shake for a further 16

hours at RT. The reaction was worked up by ethanol precipitation.

DNA ligation. Prior to ligation, the 5′ terminus of each strand was phosphorylated in separate reactions. DNA strands (Max: 450 μM, 9000 pmol in overall reaction media of 20 μL) were added PNK reaction buffer (2 μL, 500 mM Tris-HCl [pH 7.6 at 25 °C], 100 mM $MgCl_2$, 50 mM DTT, 1 mM spermidine), ATP (2 μL, 10 mM, Thermo Scientific), T4 Polynucleotide Kinase (1 μL, 10 U μL^{-1}, Thermo Scientific) and nuclease free water (up to 20 μL). The reaction was carried out at 37 °C for 1 hour, followed by heating to 75 °C for 10 min. DNA was used in the ligation steps without purification or precipitation.

Ligations contained DNA (100 μM, 9000 pmol in overall reaction media of 90 μL), phosphorylated DNA strands (Max: 20 μL, 9000 pmol), 10X T4 DNA ligase buffer (9 μL, 400 mM Tris-HCl, 100 mM $MgCl_2$, 100 mM DTT, 5 mM ATP9), water (up to 90 μL) and T4 DNA Ligase (3 μL, 30 Weiss U μL^{-1}). The ligations were carried out at 25 °C for 16 hours, followed by heating to 75 °C for 10 min. Each ligation was purified by ethanol precipitation prior to the subsequent organic reaction taking place.

BRD4 selections. An appropriate amount of His-Tag Dynabeads was washed 3 times with 100 μL of buffer and then re-suspended in the original amount of slurry. After a bead loading experiment, it was found that the loading capacity of the His-trap Dynabeads was 16 pmol BRD4 per μL of slurry. Positive beads (POS JQ1): 20 pmol of BRD4 was incubated with 1.25 μL of washed Dynabead slurry and then buffer was added up to 20 μL in Low binding tube. Negative beads (NEG JQ1): 1.25 μL of washed Dynabead slurry was diluted with buffer up to 20 μL in Low binding tube. Positive beads (POS DEL): 20 pmol of BRD4 was incubated with 1.25 μL of washed Dynabead slurry and then buffer was added up to 20 μL in Low binding tube. Negative beads (NEG DEL): 1.25 μL of washed Dynabead slurry was diluted with buffer up to 20 μL in Low binding tube. Both POS and NEG were incubated at 4 °C for 30 min on a rotating wheel. POS and NEG were then washed 3 times with 100 μL buffer and finally left dry. POS JQ1: 2 nmol of JQ1 positive control in 20 μL of buffer was added to the beads and left to incubate at 25 °C for 1 h. NEG JQ1: 2 nmol of JQ1 positive control in 20 μL of buffer was added to the beads and left to incubate at 25 °C for 1 h. POS DEL: 2 nmol of DEL-DNA in 20 μL of buffer was added to the beads and left to incubate at 25 °C for 1 h (containing 0.052 nmol of JQ1 positive control same quantity as each of the 42 members of this library). NEG DEL: 2 nmol of JQ1 positive control in 20 μL of buffer was added to the beads and left to incubate at 25 °C for 30 min (containing 0.052 nmol of JQ1-DNA same quantity as each of the 42 members of this library). POS DEL: supernatant from NEG DEL was transferred on POS DEL beads and further incubated at 25 °C for 1 h. Each sample supernatant is then removed, and beads are quickly resuspended in 20 μL ice cold buffer and then transferred in a fresh low binding tube. This step is repeated twice more. The resulting beads are then suspended in 20 μL of fresh buffer. All beads are then heated at 95 °C for 5 min. The supernatant is then immediately removed and stored in a new fresh low binding tube. The DNA outputs from the selection were amplified by qPCR (quantities listed in ESI†) and the amplified DNA were read by NGS.

Conclusions

The identification of an inhibitor with nanomolar potency in a single step from a weakly binding fragment demonstrates the power of the NUDEL poised library approach to fragment growing. Due to the careful design of the library, this also led to compounds with desirable drug like properties and cellular activity. With iterative fragment growing approaches, currently still best practice in fragment-based lead generation, reaching such an endpoint can take years and is beset with challenges associated with traversing form weakly active fragments to compounds of lead-like affinity.[26] With the availability of a NUDEL, such a goal can be achieved in mere weeks. The identification of synergistic combinations of sub-groups is enabled by the combinatorial nature of the library, the synthesis of which is often resource prohibitive with traditional off-DNA analogue exploration. Hence, as illustrated in this case, combinations of groups can be discovered that otherwise would have been highly unlikely to have been identified. This approach should be applicable to any traditional fragment library including specialised binding site mapping libraries such as MiniFrags[27] and FragLites[28,29] that return high hit rates but relatively low affinity hits. Whilst this study demonstrates the value of a small NUDEL, the same approach will be scalable to much larger libraries covering a greater degree of chemical space. We believe this approach will provide a solution to the problem of rapidly identifying potent ligands from fragment start points and become a highly valuable approach in drug discovery and chemical biology.

Data availability

Crystallographic data for **22** has been deposited at the PBD under 8C11. The datasets supporting this article have been uploaded as part of the ESI.†

Author contributions

CLAS carried out the synthesis of the NUDEL, developed the coupling reaction and carried out the selections, analysed the data and carried out subsequent chemical synthesis. BD carried out selections. JD carried out HPLC purification. MPM carried out SPR and crystallography. SJT carried out the cellular experiments. ST synthesised BRD4 protein. AK supervised BD. MEMN supervised MPM and ST. SRW supervised SJT. JC supervised CLAS. MJW conceived of the project, supervised CLAS and carried out data analysis. CLAS and MJW wrote the manuscript.

Conflicts of interest

There are no conflicts to declare.

Acknowledgements

We gratefully acknowledge the financial support of Genentech, Inc. (PhD studentship award to CLAS), EPSRC MoSMed CDT (centre funding for PhD training for CLAS, grant reference EP/S022791/1), Cancer Research UK (programme funding of the Drug Discovery Group, grant references C2115/A21421 and DRCDDRPGMApr2020\100002; Centre Network Accelerator Award, grant reference A20263); EPSRC (PhD and Doctoral Prize finding for BD, ref. EP/T517811/1); EU Horizon 2020 (fellowship awards to AK, ref. 679479 and 101003111). We thank Newcastle Structural Biology Facility and Dr. Arnaud Basle for X-ray crystallography support. We thank Emile Plise, Ivy Chen and Ruth Dorel (Genentech) for generation of ADME profiling data.

Notes and references

1 D. C. Rees, M. Congreve, C. W. Murray and R. Carr, *Nat. Rev. Drug Discovery*, 2004, **3**, 660–672.
2 C. W. Murray and D. C. Rees, *Nat. Chem.*, 2009, **1**, 187–192.
3 D. A. Erlanson, R. S. McDowell and T. O'Brien, *J. Med. Chem.*, 2004, **47**, 3463–3482.
4 D. Neri and R. A. Lerner, *Annu. Rev. Biochem.*, 2018, **87**, 479–502.
5 M. A. Clark, R. A. Acharya, C. C. Arico-Muendel, S. L. Belyanskaya, D. R. Benjamin, N. R. Carlson, P. A. Centrella, C. H. Chiu, S. P. Creaser, J. W. Cuozzo, C. P. Davie, Y. Ding, G. J. Franklin, K. D. Franzen, M. L. Gefter, S. P. Hale, N. J. V Hansen, D. I. Israel, J. Jiang, M. J. Kavarana, M. S. Kelley, C. S. Kollmann, F. Li, K. Lind, S. Mataruse, P. F. Medeiros, J. A. Messer, P. Myers, H. O'Keefe, M. C. Oliff, C. E. Rise, A. L. Satz, S. R. Skinner, J. L. Svendsen, L. Tang, K. van Vloten, R. W. Wagner, G. Yao, B. Zhao and B. A. Morgan, *Nat. Chem. Biol.*, 2009, **5**, 647–654.
6 R. A. Goodnow, C. E. Dumelin and A. D. Keefe, *Nat. Rev. Drug Discovery*, 2016, **16**, 131–147.
7 M. M. Hann, A. R. Leach and G. Harper, *J. Chem. Inf. Comput. Sci.*, 2001, **41**, 856–864.
8 A. R. Leach and M. M. Hann, *Curr. Opin. Chem. Biol.*, 2011, **15**, 489–496.
9 I. F. S. F. Castan, J. S. Graham, C. L. A. Salvini, H. A. Stanway-Gordon and M. J. Waring, *Bioorg. Med. Chem.*, 2021, **43**, 116273.
10 J.-L. Reymond, L. Ruddigkeit, L. Blum and R. van Deursen, *Wiley Interdiscip. Rev.: Comput. Mol. Sci.*, 2015, **5**, 717–733.
11 G. Schneider and U. Fechner, *Nat. Rev. Drug Discovery*, 2005, **4**, 649–663.
12 A. L. Satz, *ACS Chem. Biol.*, 2015, **10**, 2237–2245.
13 A. L. Satz, R. Hochstrasser and A. C. Petersen, *ACS Comb. Sci.*, 2017, **19**, 234–238.
14 I. J. P. de Esch, D. A. Erlanson, W. Jahnke, C. N. Johnson and L. Walsh, *J. Med. Chem.*, 2022, **65**, 84–99.
15 S. Melkko, J. Scheuermann, C. E. Dumelin and D. Neri, *Nat. Biotechnol.*, 2004, **22**, 568–574.
16 G. Bassi, N. Favalli, M. Vuk, M. Catalano, A. Martinelli, A. Trenner, A. Porro, S. Yang, C. L. Tham, M. Moroglu, W. W. Yue, S. J. Conway, P. K. Vogt, A. A. Sartori, J. Scheuermann and D. Neri, *Adv. Sci.*, 2020, **7**, 2001970.
17 M. Catalano, M. Moroglu, P. Balbi, F. Mazzieri, J. Clayton, K. H. Andrews, M. Bigatti, J. Scheuermann, S. J. Conway and D. Neri, *ChemMedChem*, 2020, **15**, 1752–1756.
18 S. Puglioli, E. Schmidt, C. Pellegrino, L. Prati, S. Oehler, R. De Luca, A. Galbiati, C. Comacchio, L. Nadal, J. Scheuermann, M. G. Manz, D. Neri, S. Cazzamalli, G. Bassi and N. Favalli, *Chem*, 2023, **9**, 411–429.
19 J. H. Hunter, L. Prendergast, L. F. Valente, A. Madin, G. Pairaudeau and M. J. Waring, *Bioconjugate Chem.*, 2020, **31**, 149–155.
20 J. H. Hunter, M. Potowski, H. A. Stanway-Gordon, A. Madin, G. Pairaudeau, A. Brunschweiger and M. J. Waring, *J. Org. Chem.*, 2021, **86**, 17930–17935.
21 J. S. Graham, J. H. Hunter and M. J. Waring, *J. Org. Chem.*, 2021, **86**, 17257–17264.
22 D. S. Hewings, M. Wang, M. Philpott, O. Fedorov, S. Uttarkar, P. Filippakopoulos, S. Picaud, C. Vuppusetty, B. Marsden, S. Knapp, S. J. Conway and T. D. Heightman, *J. Med. Chem.*, 2011, **54**, 6761–6770.
23 P. Filippakopoulos, J. Qi, S. Picaud, Y. Shen, W. B. Smith, O. Fedorov, E. M. Morse, T. Keates, T. T. Hickman, I. Felletar, M. Philpott, S. Munro, M. R. McKeown, Y. Wang, A. L. Christie, N. West, M. J. Cameron, B. Schwartz, T. D. Heightman, N. La Thangue, C. A. French, O. Wiest, A. L. Kung, S. Knapp and J. E. Bradner, *Nature*, 2010, **468**, 1067–1073.
24 J. E. Delmore, G. C. Issa, M. E. Lemieux, P. B. Rahl, J. Shi, H. M. Jacobs, E. Kastritis, T. Gilpatrick, R. M. Paranal, J. Qi, M. Chesi, A. C. Schinzel, M. R. McKeown, T. P. Heffernan, C. R. Vakoc, P. L. Bergsagel, I. M. Ghobrial, P. G. Richardson, R. A. Young, W. C. Hahn, K. C. Anderson, A. L. Kung, J. E. Bradner and C. S. Mitsiades, *Cell*, 2011, **146**, 904–917.
25 R. J. Young and P. D. Leeson, *J. Med. Chem.*, 2018, **61**, 6421–6467.
26 M. P. Martin and M. E. M. Noble, *Acta Crystallogr., Sect. D: Struct. Biol.*, 2022, **78**, 1294–1302.
27 M. O'Reilly, A. Cleasby, T. G. Davies, R. J. Hall, R. F. Ludlow, C. W. Murray, D. Tisi and H. Jhoti, *Drug Discovery Today*, 2019, **24**, 1081–1086.
28 D. J. Wood, J. D. Lopez-Fernandez, L. E. Knight, I. Al-Khawaldeh, C. Gai, S. Lin, M. P. Martin, D. C. Miller, C. Cano, J. A. Endicott, I. R. Hardcastle, M. E. M. Noble and M. J. Waring, *J. Med. Chem.*, 2019, **62**(7), 3741–3752.
29 G. Davison, M. P. Martin, S. Turberville, S. Dormen, R. Heath, A. B. Heptinstall, M. Lawson, D. C. Miller, Y. M. Ng, J. N. Sanderson, I. Hope, D. J. Wood, C. Cano, J. A. Endicott, I. R. Hardcastle, M. E. M. Noble and M. J. Waring, *J. Med. Chem.*, 2022, **65**(22), 15416–15432.